The contrasting activity of iodido versus chlorido ruthenium and osmium arene azo- and imino-pyridine anticancer complexes: control of cell selectivity, cross-resistance, p53 dependence, and apoptosis pathway. — **Source link** ↗

Isolda Romero-Canelón, Luca Salassa, Peter J. Sadler

Institutions: University of Warwick, Coventry Health Care

Topics: Cisplatin

Related papers:

- Inhibition of cancer cell growth by ruthenium(II) arene complexes

- A short history of SHELX

- The resurgence of platinum-based cancer chemotherapy

- Arene ruthenium complexes as anticancer agents

- In Vitro and in Vivo Evaluation of Ruthenium(II)−Arene PTA Complexes

Share this paper: f 𝕏 in ✉

View more about this paper here: https://typeset.io/papers/the-contrasting-activity-of-iodido-versus-chlorido-ruthenium-34j8j9s3mn

THE UNIVERSITY OF
WARWICK

For more information, please contact the WRAP Team at: wrap@warwick.ac.uk
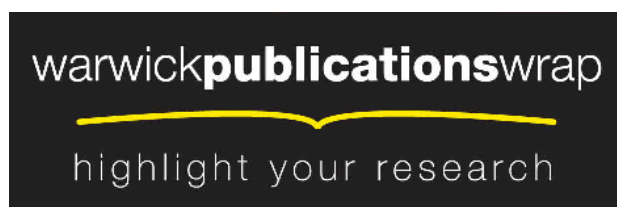
warwick**publications**wrap

highlight your research

http://go.warwick.ac.uk/lib-publications

The Contrasting Activity of Iodido versus Chlorido Ruthenium and Osmium Arene Azo- and Imino-pyridine Anticancer Complexes: Control of Cell Selectivity, Cross-Resistance, p53 Dependence, and Apoptosis Pathway

Isolda Romero-Canelón,[†] Luca Salassa,[†,‡] and Peter J. Sadler*,[†]

[†]Department of Chemistry, University of Warwick, Library Road, CV4 7AL Coventry, U.K.
[‡]CIC BiomaGUNE, Paseo Miramon 182, 20009 Donostia, San Sebastián, Spain

Ⓢ *Supporting Information*

ABSTRACT: Organometallic half-sandwich complexes [M(*p*-cymene)(azo/imino-pyridine)X]$^+$ where M = Ru^{II} or Os^{II} and X = Cl or I, exhibit potent antiproliferative activity toward a range of cancer cells. Not only are the iodido complexes more potent than the chlorido analogues, but they are not cross-resistant with the clinical platinum drugs cisplatin and oxaliplatin. They are also more selective for cancer cells versus normal cells (fibroblasts) and show high accumulation in cell membranes. They arrest cell growth in G1 phase in contrast to cisplatin (S phase) with a high incidence of late-stage apoptosis. The iodido complexes retain potency in p53 mutant colon cells. All complexes activate caspase 3. In general, antiprolifera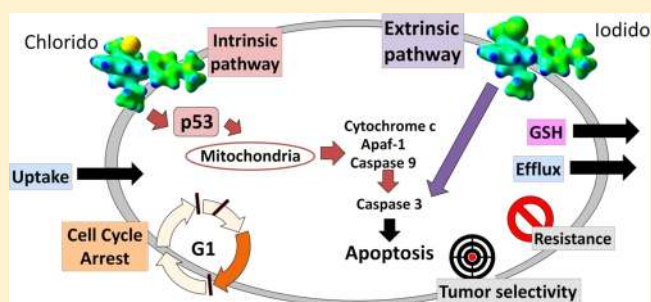tive activity is greatly enhanced by low levels of the glutathione synthase inhibitor L-buthionine sulfoxime. The work illustrates how subtle changes to the design of low-spin d^6 metal complexes can lead to major changes in cellular metabolism and to potent complexes with novel mechanisms of anticancer activity.

INTRODUCTION

Since the introduction of cisplatin (CDDP) into the clinic about 40 years ago, Pt-based drugs CDDP, carboplatin, and oxaliplatin (OXA) have become the most widely used anticancer agents (about 50% of therapeutic regimes). However only recently has understanding of their mechanism of action begun to emerge.[1−4] The problems of platinum resistance and undesirable side-effects are stimulating the search for alternative transition metal anticancer drugs, and two Ru^{III} complexes are now in clinical trials.[5] Ruthenium(III) complexes are likely to be activated by reduction to Ru^{II} in the body and a range of highly active organometallic Ru^{II} anticancer complexes have been reported.[6−8] However future success in optimizing the design of metal-based therapeutic compounds depends greatly on understanding their cellular metabolism[9,10] and mechanisms of action.

Small changes in the structure of metal complexes can have a major effect on biological activity. It was found in the early days after the discovery of the anticancer activity of CDDP that replacement of the chlorido ligands to give the diiodido complex *cis*-[PtI$_2$(NH$_3$)$_2$] completely abolished the activity.[11] Since that report, there have been few studies of the effects of Cl−I substitutions on the activity of transition metal complexes, although active *trans* Pt^{II} diamine diiodido complexes have been recently reported.[12] Here we show that the cellular metabolic pathways for organometallic Ru^{II} and Os^{II} arene anticancer

complexes are dramatically altered by the replacement of coordinated chloride by iodide in both iminopyridine and azopyridine complexes, with surprising advantages for complexes containing an iodido ligand. This has been demonstrated by investigating the antiproliferative activity, metal accumulation and distribution in cancer cells, cell cycle analysis, p53-dependence, apoptosis, caspase 3 activation, and redox modulation, of [M(*p*-cymene)(azo/imino-pyridine)X]$^+$ complexes where M = Ru^{II} or Os^{II}, and X = Cl or I.

RESULTS AND DISCUSSION

We have investigated the antiproliferative activity and cellular mechanism of action of six closely related "half-sandwich", "piano-stool", pseudo-octahedral organometallic complexes with the same π-bound arene (*p*-cymene) but differing only in their chelated ligand (azopyridine or isoelectronic iminopyridine) or in the monodentate ligand (chloride or iodide). These subtle variations in the structures of the complexes have dramatic effects on their cellular properties.

The structural features of organometallic Ru^{II} "piano-stool" complexes allow fine-tuning of their physical and chemical properties and optimization of their biological activity.[5,13−15] These complexes contain three basic building blocks as shown

in Figure 1: an arene ligand (the "seat" of the "stool"), used to control hydrophobicity and to stabilize the oxidation state of

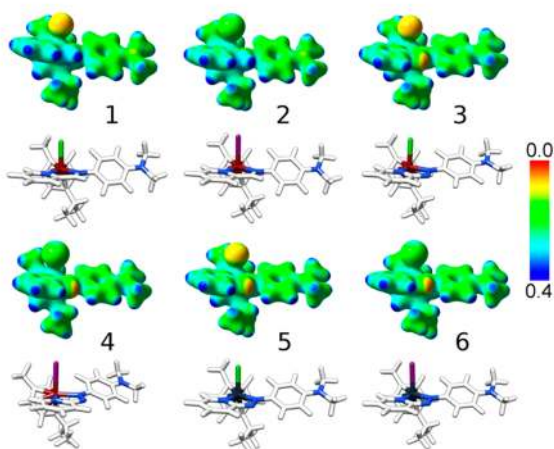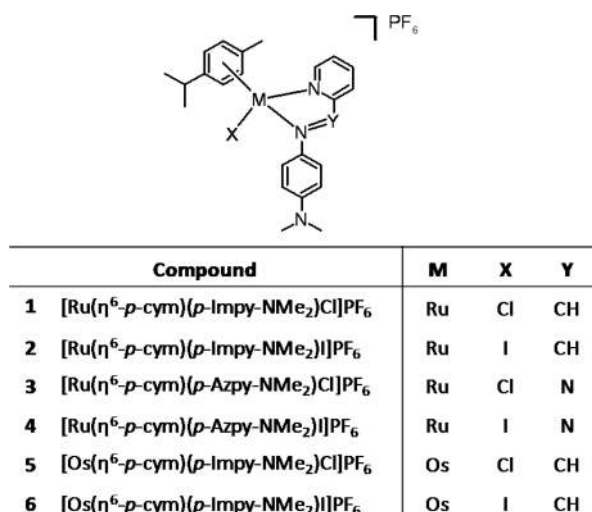|	Compound	M	X	Y
1	[Ru(η^6-p-cym)(p-Impy-NMe$_2$)Cl]PF$_6$	Ru	Cl	CH
2	[Ru(η^6-p-cym)(p-Impy-NMe$_2$)I]PF$_6$	Ru	I	CH
3	[Ru(η^6-p-cym)(p-Azpy-NMe$_2$)Cl]PF$_6$	Ru	Cl	N
4	[Ru(η^6-p-cym)(p-Azpy-NMe$_2$)I]PF$_6$	Ru	I	N
5	[Os(η^6-p-cym)(p-Impy-NMe$_2$)Cl]PF$_6$	Os	Cl	CH
6	[Os(η^6-p-cym)(p-Impy-NMe$_2$)I]PF$_6$	Os	I	CH

Figure 1. Structures and electrostatic potential surfaces (EPSs) for organometallic Ru[II] complexes **1**−**4** and Os[II] complexes **5** and **6**. EPS surfaces are shown in both space and mapped on electron density (isovalue 0.04) of the molecules. The electrostatic potential is represented with a color scale going from red (0.0 au) to blue (0.40 au).

the metal center, a monodentate ligand, X, initially included as an activation site, and a bidentate ligand which provides additional stability.[16,17] Such complexes can often undergo activation by aquation, the loss/replacement of the monodentate ligand[16] and subsequent binding to DNA nucleobases such as guanine and adenine[18] or even conjugation to glutathione followed by oxidation to the sulfenate and then DNA binding.[19,20]

Complexes [Ru(η^6-p-cym)(p-Impy−NMe$_2$)Cl]PF$_6$ (**1**) and [Ru(η^6-p-cym)(p-Impy−NMe$_2$)I]PF$_6$ (**2**) were synthesized and characterized as described in the Experimental Section, while complexes [Ru(η^6-p-cym)(p-Azpy-NMe$_2$)Cl]PF$_6$ (**3**),[21] [Ru-(η^6-p-cym)(p-Azpy-NMe$_2$)I]PF$_6$ (**4**)[21] and [Os(η^6-p-cym)(p-Impy−NMe$_2$)Cl]PF$_6$ (**5**),[22] [Os(η^6-p-cym)(p-Impy−NMe$_2$)I]-PF$_6$ (**6**)[22] were obtained as previously reported. These complexes contain either iminopyridine (**1**, **2**, **5**, **6**) or isoelectronic azopyridine (**3**, **4**) as the *N,N*-chelator, and chloride (**1**, **3**, **5**) or iodide (**2**, **4**, **6**) as monodentate ligand. Complexes **5** and **6** are the Os[II] analogues of the Ru[II] complexes **1** and **2**. ^{1}H NMR experiments in D$_2$O (Supporting Information) show that 2 mM solutions of complexes **1** and **2** in water aquate (replacement of halide by water) to a similar extent over 24 h, 66% and 63%, respectively. Complex **3** aquates to an extent of 55% in the same time, while the iodido complex **4** is inert and does not form an aqua complex under these conditions.[21] Aquation of the osmium analogues was also studied; chlorido complex **5** aquates 50% after 24 h, and complex **6** is fully converted to the aqua species in the same time[22] (Supporting Information Table S1). However, this aquation reaction was totally inhibited by the presence of chloride ions. Also, ^{1}H NMR experiments showed that complexes **1** and **2** do not aquate after 24 h at 298 K when dissolved in RPMI-1640 medium (Supporting Information). This cell culture medium contains NaCl at a concentration of 108 mM, close to blood plasma chloride concentration (ca. 104 mM),[23] suggesting that these complexes do not aquate before they enter cells. The ^{1}H NMR data suggest that complex **2** is stable after 48 h in the cell culture medium.

It was also important for this work to establish that the iodido complexes are not readily converted into the chlorido analogues in the cell culture medium by ligand exchange. Because of the high chloride levels, the possibility that the iodido ligand in complexes **2**, **4**, and **6** could be substituted by chloride was investigated. HPLC studies (Supporting Information) showed that after incubation of complex **2** with 150 mM NaCl at 310 K for 24 h, there was <5% substitution of the iodide ligand by chloride.

Table 1. Antiproliferative Activity of Complexes 1−6, CDDP, and OXA in A2780, A549, HCT116, and MCF7 Cell Lines and Cellular Accumulation of Ru/Os in A2780 Cells after 24 h of Drug Exposure at 310 K[a]

	IC$_{50}$ (μM)				cell accumulation
	A2780	A549	HCT116	MCF7	A2780
1	16.2 ± 0.9	10.5 ± 0.8	3.4 ± 0.4	12.1 ± 0.3	7.8 ± 0.5
2	3.0 ± 0.2	15.3 ± 0.9	8.6 ± 0.8	4.4 ± 0.3	11.5 ± 0.8
3	13.1 ± 0.5	15 ± 1	16.7 ± 0.8	11.9 ± 0.9	13.4 ± 0.9
4	0.69 ± 0.04	1.27 ± 0.01	1.37 ± 0.04	0.8 ± 0.1	17.9 ± 0.8
5	3.0 ± 0.4	15.8 ± 0.2	3.26 ± 0.05	9.3 ± 0.6	15.2 ± 0.9
6	1.20 ± 0.02	3.31 ± 0.6	1.6 ± 0.1	1.2 ± 0.2	18.1 ± 0.1
CDDP	1.2 ± 0. 2	3.3 ± 0.1	5.1 ± 0.3	7.4 ± 0.2	nd
OXA	nd	nd	3.99 ± 0.08	nd	nd

[a]Cell accumulation experiments did not include recovery time in drug free media. Results are expressed as ng Ru/Os per 10^6 cells, and the concentrations used were equipotent, in all cases IC$_{50}$/3. nd = not determined.
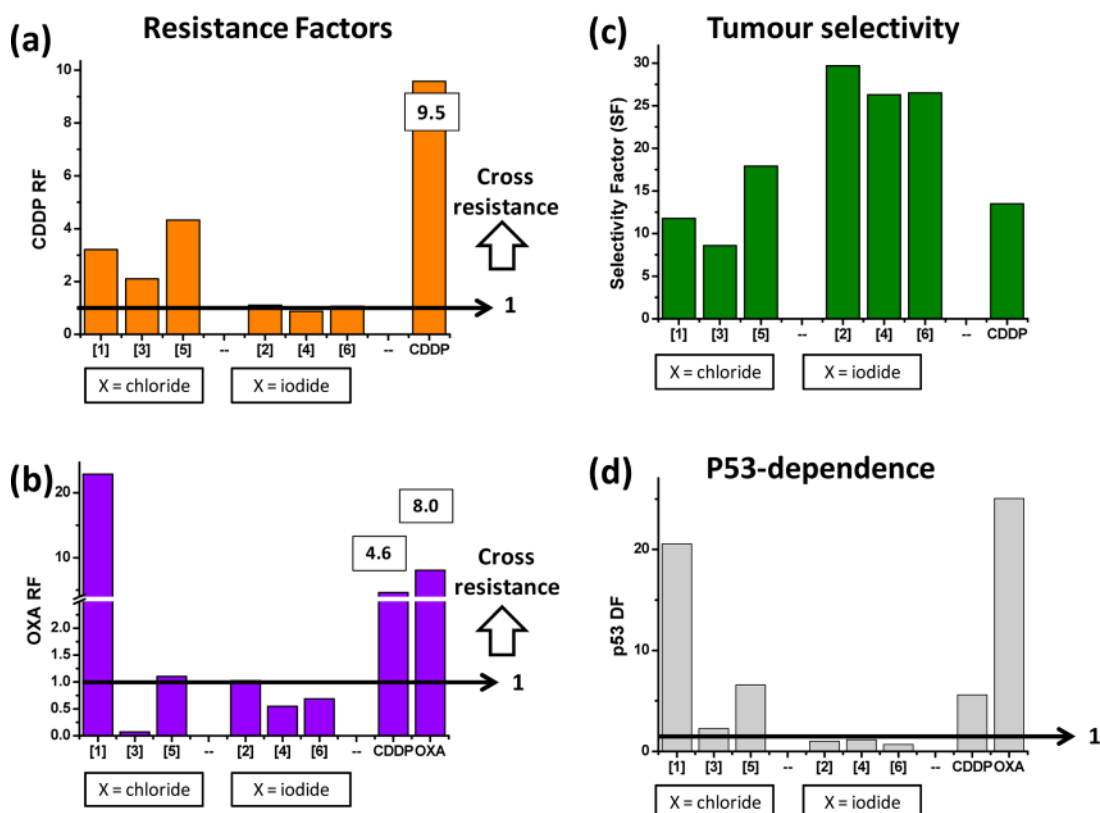
Figure 2. (a) Resistance factors, RF, for complexes **1**−**6** toward CDDP-resistant A2780 human ovarian cancer cells (A2780cis). (b) RF values toward OXA-resistant HCT116 human colon cancer cells (HCT116Ox) in comparison with CDDP and OXA. (c) Tumor selectivity factors, SF between MRC5 human fibroblasts and A2780 human ovarian cancer cells. (d) p53-dependence factors, DF between HCT116 human colon cancer cells and p53 knocked out mutants. In all cases, data shown are the ratio of IC_{50} values in the modified cell line and the parental line. Cells were exposed to complexes **1**−**6** for 24 h at 310 K.

Electronic Structures of Iodido and Chlorido Complexes. Geometries and electronic structures of complexes **1**−**6** were calculated using the DFT method at the PBE0/Lanl2DZ/6-311G** level.[24−26] With the exception of the metal−halogen bonds, only very minor differences are observed in the bond distances for complexes **1**−**6**. Notably, electrostatic potential surfaces (EPSs) clearly show a difference in charge distribution between chlorido and iodido complexes regardless of the metal center or chelating ligand (Figure 1). The rather flat color distribution in the EPSs of **1**−**6** indicates that the metal complexes are relatively nonpolar. However, all chlorido complexes display a more polarized metal−halogen bond, with the chlorido ligand being less positively charged than the iodido ligand (Supporting Information Tables S2, S3).

Antiproliferative Activity. The IC_{50} values for complexes **1**−**6** in A2780 ovarian, A549 lung, HCT116 colon, and MCF7 breast carcinoma cells were determined (Table 1). All complexes are highly active in all parental cell lines (IC_{50} values <17 μM), especially azopyridine iodido ruthenium complex **4**, which exhibits submicromolar activity in A2780 and MCF7 cell lines and is, in all cases, more potent than CDDP. Iodido complexes **4** and **6** are more potent than their chlorido analogues **3** and **5** in all cell lines. Complex **4** is between 12× and 19× more potent than **3**, while the difference between **6** and **5** ranges between 2× and 7×.

Changes in the monodentate ligand can modify the cellular uptake and accumulation pathways involved in the first stages of drug action. This leads to variations in cellular distribution of the drug and, in turn, to different apoptotic pathways being triggered as a consequence of cellular compartmentalization,[27] hence determining differences in IC_{50} values. Substitution of the metal is likely to be the cause of the increase in potency of the osmium p-Impy−NMe2 complexes compared to their ruthenium analogues (with the exception of chlorido complex **5** in A549 cells). This substitution changes the redox potential of the complex, which in turn can be related to the generation of ROS and modifications of mitochondrial activity.[28,29] Generated secondary species generally exhibit reduction potentials amenable to electron transfer in vivo, thus giving rise to ROS.[30] Electrochemical reduction at −0.40 V has previously been found[21] for ruthenium complex **4**, a value within the biologically relevant range (+0.40 to −0.50 V),[30] making possible its involvement in mitochondrial activity.

To investigate whether free iodido ions, if released from complexes **2**, **4**, or **6**, might also play a role in activity, we determined the IC_{50} value of chlorido complex **1** for A2780 cells in the presence of an equimolar amount of KI. The antiproliferative activity of this mixture (IC_{50} = 16.6 ± 0.4 μM) was the same as in the absence of added iodide (IC_{50} = 16.2 ± 0.9 μM for complex **1** only). These data are consistent with the conclusion that the difference in biological activity of the iodido complexes arises from the different targeting properties of the complexes with Ru−I compared to Ru−Cl bonds and also consistent with the experimental observation that intact iodido complex **2** enters cells.

Iodido Complexes Are Not Cross-Resistant with CDDP or OXA. The activity of complexes **1**−**6** toward CDDP-resistant A2780 ovarian (A2780 Cis) and OXA-resistant

HCT116 colon (HCT116Ox) cancer cells was investigated. Chlorido complexes **1**, **3**, and **5** share partial cross-resistance with CDDP, although the resistance factor, RF, drops from 9.5 for CDDP to between 2 and 5 for the chlorido complexes (Figure 2a and Supporting Information Table S4). In dramatic contrast, the iodido complexes **2**, **4**, and **6** retain their potency in CDDP-resistant A2780 Cis cells (RF $\cong$ 1). Remarkably, all cross-resistance factors are lower than for CDDP, which could give rise to a clinical advantage for the arene half-sandwich complexes.

One common clinical strategy to treat cancers that have acquired resistance to CDDP is the use of OXA, even though the mechanism of action of this platinum-based metallo-drug shares some features with that of CDDP. This clinical approach is especially important in the treatment of colorectal cancer, with the common consequence of acquired resistance to both platinum drugs. Iodido complexes **2**, **4**, and **6** also retain their full potency toward OXA-resistant colon cancer cells HCT116Ox, which show an RF of 8.0 for OXA itself (Figure 2b). Once again this suggests differences in the mechanism of action of these arene complexes compared to that of OXA. In contrast, chlorido complex **1** is highly cross-resistant (RF = 22.8), whereas, curiously, **3** is much more potent (RF = 0.07), while **5** retains activity (RF = 1.1). It is notable that CDDP (RF = 4.6) and OXA show cross-resistance in this cell line. CDDP and OXA react with GC-rich sites in DNA and are believed to form mainly intrastrand cross-links.[31] However it has been reported that OXA requires lower intracellular concentrations and fewer DNA-Pt adducts to cause the same extent of cell death than CDDP.[31] Both produce early SSB (single-strand breaks), but it has been suggested that although more early lesions are caused by CDDP, it is OXA which generates lesions that are more difficult to repair, as they are not recognized by MMR (mismatch repair) proteins.[32]

Iodido Complexes Are More Cell-Selective than CDDP. Differential selectivity of an anticancer drug toward cancer cells versus normal cells increases the likelihood of tumor-specific cytotoxicity, so reducing side-effects in patients. We chose MRC5 fibroblasts as normal cells because they are often used to evaluate the tissue selectivity of chemotherapeutic drugs, especially of natural origin,[33] and also photodynamic therapy agents.[34] The cell selectivity factors (SF = ratio of IC_{50} for MRC5 human lung fibroblasts/IC_{50} for A2780 cells) for the chlorido complexes **1** (SF = 11.8), **3** (SF = 8.5), and **5** (SF = 17.9) are comparable or higher than that of CDDP (SF = 9.5). Importantly the iodido complexes **2**, **4**, and **6** are significantly more selective, with SF values >26 (Figure 2c and Supporting Information Table S4).

High Cell Accumulation of Potent Iodido Complexes. The extent of ruthenium or osmium accumulation in A2780 cells was determined for complexes **1**–**6** (Table 1) to investigate a possible correlation with antiproliferative activity. In general, higher metal accumulation is associated with higher potency (Supporting Information Figure S1). The most potent complexes, **4** (Ru) and **6** (Os), both iodido, are associated with >2× the cell accumulation of metal compared to the least active complex **1**. The Ru iodido complex **2** has notably higher activity than would be expected from its extent of accumulation and, in contrast, the Ru chlorido complex **3** has a lower activity than might be expected on the basis of metal accumulation alone. Differences in cellular accumulation cannot be explained by differences in the extent of aquation/halide exchange for the complexes.

Contrasting Subcellular Distributions of Chlorido and Iodido Complexes. The distribution of metal (Ru/Os) in four cellular fractions was studied (Figure 3 and Supporting
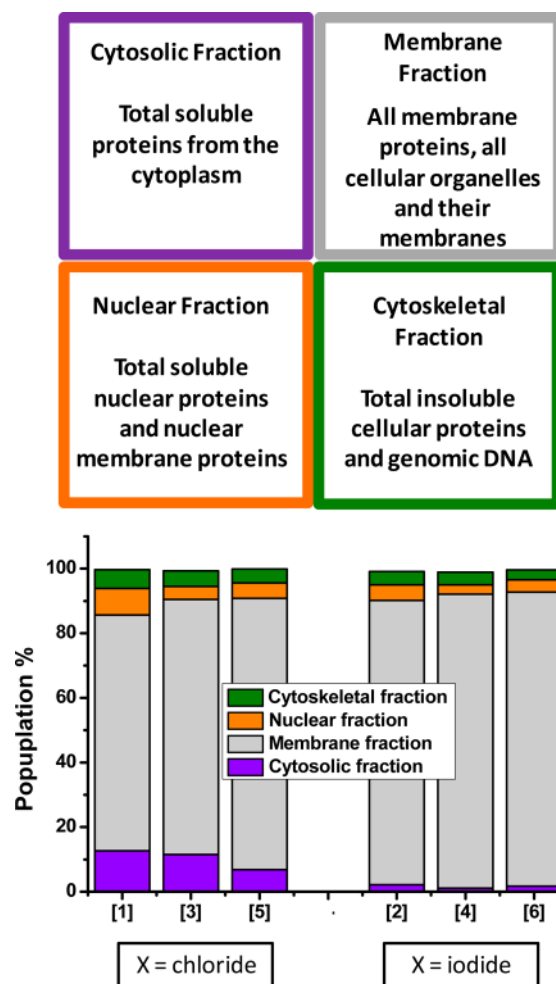

Figure 3. Distribution of metal (Ru/Os) in A2780 human ovarian cancer cells after 24 h exposure to complexes **1**–**6** at 310 K. Concentrations were equipotent at $IC_{50}/3$.

Information Table S5); Complexes **1**–**6** all accumulate to a high extent in the membrane fraction which contains membrane proteins, cellular organelles, and organelle membranes. The percentage of metal from the iodido complexes **2**, **4**, and **6** in the membrane fraction is slightly higher (ca. 88–91%) than for their chlorido analogues **1**, **3**, and **5** (ca. 73–84%). It is also notable that there is little accumulation of the metal from the iodido complexes in the cytosolic fraction (<2%) which includes the total soluble proteins from the cytoplasm. The differences in cellular metal distribution can be attributed to differences in the cellular pathways involved in the uptake and efflux of these complexes.[35] Moreover, this difference in distribution may determine the apoptotic pathways which they activate. This is consistent with recent studies that have linked endocytosis pathways to cellular signal transduction, suggesting bidirectional interplay between the two processes,[27] moreover, cellular compartmentalization can induce selective transmission of signals that can lead either to apoptosis or survival of the cell.[36,37]

Cell Cycle Arrest in G1 in Contrast to CDDP. In comparison to the control population, the cell cycle data

(Figure 4 and Supporting Information Table S6) clearly show that CDDP causes arrest in the S phase. The population in this
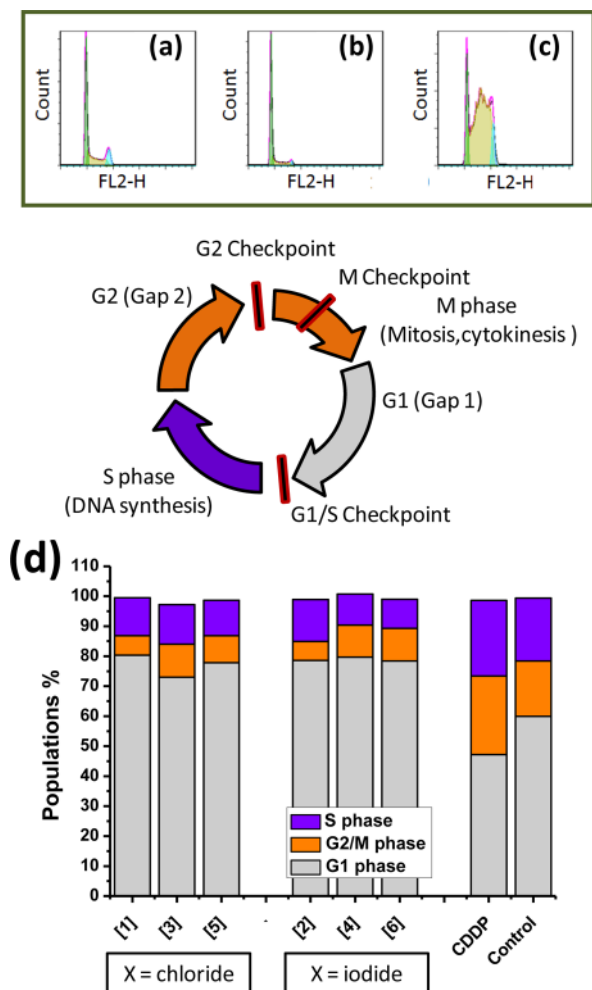

Figure 4. Cell cycle analysis of A2780 human ovarian cancer cells after 24 h of exposure to complexes **1–6** at 310 K. Concentrations used were equipotent at IC$_{50}$/3. Cell staining for flow cytometry was carried out using PI/RNase. (a) FL2 histogram for negative control: cells untreated. (b) FL2 histogram for cells exposed to complex **2**, 1 μM. (c) FL2 histogram for cells exposed to CDDP, 0.4 μM. (d) Populations in each cell cycle phase for complexes **1–6**.

phase increases after 24 h of exposure to the Pt drug, together with a significant reduction in the population in G1 phase, in agreement with previous reports.[38] In contrast, complexes **1–6** cause arrest in G1 phase (ca. 69–80%) regardless of the nature of their metal center (Ru/Os) or the monodentate ligand (Cl/I). Interestingly, Impy–NMe$_2$ complexes **1** and **2**, in contrast to Azpy–NMe$_2$ complexes **3** and **4**, caused the S phase population to be twice as large as the G2/M population.

Hence complexes **1–6** do not allow A2780 cells to progress into the division phase of the cell cycle. G1 arrest has previously been reported for some other ruthenium(II) complexes.[39] Interestingly, Ru–Impy complexes **1** and **2** may interfere with DNA and/or chromosome replication, as cells are partially retained in the second checkpoint which checks for DNA damage. CDDP attacks DNA which triggers cell cycle arrest and does not allow progression into cell division. Some cancer treatments currently in clinical use are known to exploit G1 arrest. For example, Clotrimazole induces a late G1 cell cycle

arrest and sensitizes glioblastoma cells to radiation in vitro.[40] Also Paclitaxel causes G1 arrest in A549 lung cancer cells at low concentrations (3−6 nM); it inhibits cell proliferation by activation of p53 and p21 without arresting cells at mitosis.[41]

For CDDP, S phase arrest is concentration-dependent (Supporting Information Table S7). At higher concentrations of the Pt drug, the number of DNA-Pt lesions increases, making the repair process slower and inefficient. This holds a greater population of cells in S phase. In contrast, cell cycle arrest by Ru complex **2** is concentration-independent (Supporting Information Table S8); the population arrested in G1 phase does not increase significantly with the concentration of the complex. This may provide an advantage for an anticancer drug, as the cytostatic activity will occur even at low drug concentrations.

Iodido Complexes Retain Potency in p53 Mutant Cells. Disruption of the p53 pathway has been strongly correlated with tumorigenesis, as it is considered to maintain genomic stability. Inactivation of p53 is the most common event in human cancers, occurring in at least 50% of all cases.[42,43] The antiproliferative activity of complexes **1–6** toward HCT116 colon cancer cells was determined and compared to that in the derived cell line HCT116p53−/− which has knocked out tumor suppressor p53 (Supporting Information Table S4). It is remarkable that the differences in the IC$_{50}$ values in HCT116p53−/− for complexes **1–6** seem to be associated with the halide present as the monodentate ligand and not with the metal center, nor the *N,N*-chelating ligand.

Figure 3d shows the dependence of antiproliferative activity on the presence of p53, expressed as DF, the ratio of the IC$_{50}$ in the parental cell line to IC$_{50}$ in the cell line with p53 knocked out. The DF values for complexes **2**, **3**, **4**, and **6** are close to 1, which indicates that the activity of these complexes is independent of the p53 status. The cytotoxicity of ruthenium *p*-Impy−NMe$_2$ complex **1**, for which the IC$_{50}$ value increases ca. 17× (from 3.4 ± 0.4 to 69.9 ± 0.9 μM) and complex **5** with potency loss from 3.26 ± 0.05 to 21.5 ± 0.8 μM, evidently both depend on activation of p53. Activation of p53, by DNA damage, cytotoxic drugs, hypoxia, or oncogenic signaling among others, is known to cause cell cycle arrest in G1 phase as well as being involved in the intrinsic apoptotic pathway.[44]

G1 arrest observed for complexes **1** and **5** may be related to their p53 dependence. It is possible that the chlorido complexes **1** and **5** activate p53, which in turns arrests the cell cycle, so when p53 is knocked out in HCT116 cells, the arrest does not occur and cell proliferation increases, which is manifested as an increase in the IC$_{50}$ value.

Iodido complexes **2**, **4**, and **6** are as potent in the p53-null cell line as in the parental line (Figure 3d). This suggests that their mechanism of action does not involve the intrinsic apoptotic pathway. Drugs with a mechanism of action independent of p53 status might be advantageous for clinical use, especially because the treatment of choice for colon cancer is OXA, which shows an IC$_{50}$ above 100 μM and a dramatic potency loss in the HCT116p53−/− cell line (DF >25, Figure 3d). Similar results are obtained for CDDP, which is 5× less potent in the HCT166p53−/− cell line (IC$_{50}$ 36.7 ± 0.3 versus 5.1 ± 0.3 μM). Other ruthenium complexes have been previously studied in relation to their p53-dependence,[45] particularly, chlorido complex [Ru(η^6-biphenyl)-(ethylenediamine)Cl]$^+$ (RM175), which activates p53-dependent pathways.[46]

The Cytostatic Switch: Apoptosis for Iodido Complexes Is Late Stage. Morphological changes in early apoptotic cells usually involve the loss of phospholipid asymmetry followed by the translocation of phosphatidylserine to the outer membrane. The phospholipid component is normally found on the internal/cytosolic side of the membrane in healthy cells. This protein translocation is key for the detection of apoptosis by annexin V.[47] In late stages of apoptosis, the membrane is totally compromised as the cell breaks apart into several vesicles or apoptotic bodies. In the process, membrane blebbing allows formerly impermeant agents, like propidium iodide (PI), to access inner cell compartments.

The extent of apoptosis for A2780 cells caused by complexes **1**−**6** was investigated by flow cytometry (Figure 5). These
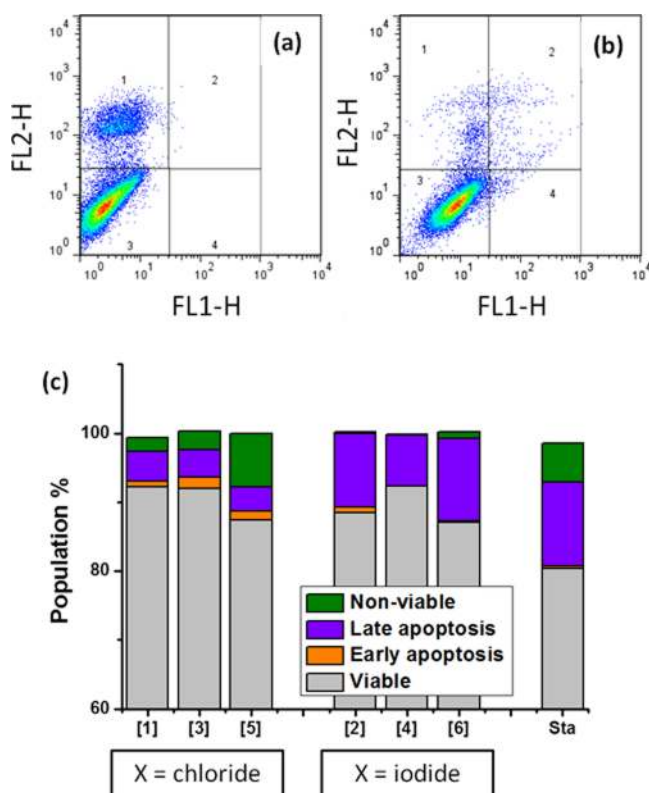

Figure 5. Apoptosis analysis of A2780 human ovarian cells after 24 h of exposure to complexes **1**−**6** at 310 K determined by flow cytometry using Annexin V-FITC vs PI staining. (a) FL1 vs FL2 histogram for cells exposed to staurosporine, 1 μM. (b) FL1 vs FL2 histogram for cells exposed to complex **2**, 1 μM. (c) Populations for complexes **1**−**6**.

arene half-sandwich complexes cause apoptosis but differ in the time frame of the process (Figure 4 and Supporting Table S8). The iodido complexes **2**, **4**, and **6** exhibit a high incidence of late apoptotic cells (ca. 7−12%) after 24 h of exposure compared to the chlorido complexes (ca. 3.5−4%). Notably the population of nonviable cells caused by the iodido complexes is very low (ca. 0.10−0.95%). In contrast, the chlorido complexes **1**, **3**, and **5** give rise to early stage apoptosis after the same time of exposure to drug and also produce a higher population of nonviable cells (ca. 2−8%). These differences might indicate that although all complexes activate apoptotic cascades, the processes involving iodido complexes are different from those involving chlorido analogues generating variations in the time each pathway takes to cause cell death.

Enhanced Activation of Caspase 3 by Chlorido Complexes. Caspases, in general, are a family of cysteine proteases that play essential roles in apoptosis, necrosis, and inflammation.[48] Caspase 3, in particular, also known as CPP32, is encoded by the CASP3 gene in humans and recognizes the peptide sequence DEVDG (Asp-Glu-Val-Asp-Gly), with cleavage occurring on the carboxyl side of the second aspartic acid residue. Colorimetric methods can be used to measure its activation when the DEVD sequence is labeled with p-NA.[49]

The effect of complexes **1**−**6** on the activation of caspase 3 in A2780 cells was monitored spectrophotometrically using the substrate DEVD-pNA. All these arene complexes activate caspase 3. Remarkably, the level of activation of caspase 3 by the chlorido complexes **1**, **3**, and **5** is 2-fold higher than by the iodido complexes **2**, **4**, and **6** (Supporting Information Table S9 and Figure S3).

Polypyridyl ruthenium complexes have also been reported to induce apoptosis with activation of caspase 3 via the intrinsic pathway.[50] Interestingly, anticancer agents that interact with DNA, specifically with mitochondrial DNA (mDNA), selectively enhance the generation of ROS in mitochondria and the release of cytochrome c, inducing apoptosis after activating caspases 9 and 3.[51] Cell compartmentalization studies showed that complexes **1**−**6** accumulate highly in the membrane fraction that includes the mitochondria, and they also activate caspase 3.

Redox Modulators Increase Potency. Complexes **1**−**6** were coadministered with L-buthionine sulfoximine (L-BSO) to investigate the role of GSH in the cellular detoxification of these organometallic complexes. L-BSO is a specific inhibitor of γ-glutamylcysteine synthetase which is involved in the rate-limiting step in the synthesis of GSH. Thus treatment with L-BSO can significantly decrease intracellular GSH levels. When used as a single agent in high concentrations, L-BSO is capable of increasing ROS levels, causing apoptosis.[52] However, it has also been used at low doses to increase the sensitivity to certain anticancer drugs that depend on GSH-mediated detoxification.[53] L-BSO has been included in phase I clinical trials and appears to be safe to the point of reducing GSH levels by 40%.[54]

The potency of all the complexes increased when coincubated with 5 μM L-BSO (Supporting Information Table S10 and Figure S2), especially complexes **1**, **3**, and **6**, for which the IC$_{50}$ values decreased by factors of 16, 8, and 15, respectively, while for complexes **2**, **4**, and **5**, the increase in potency ranged from 2.8× to 7.1×. Inhibition of detoxification mechanisms by administration of L-BSO has been used previously as a strategy to increase the activity of a range of metal-based drugs.[55,56] For example, L-BSO partially restores sensitivity to CDDP in several resistant cancer cell lines and improves the activity of ruthenium(III) complexes such as KP1019.[28] An increase in intracellular GSH levels provides one mechanism for CDDP resistance, and platinum binds strongly and irreversibly to the thiolate sulfur of GSH, so inhibiting binding to DNA.[1]

■ CONCLUSIONS

Our results show that switching the halido ligand in ruthenium and osmium arene azo- and imino-pyridine complexes can tune their antiproliferative activity with strong repercussions at the molecular level. There may be clear advantages in using iodido complexes for future clinical applications as they do not share

mechanisms of resistance with CDDP nor OXA and their activity does not depend on the status of p53 tumor suppressor.

Halide switch from chloride to iodide increases the polarization of positive charge on the chelated face of these pseudo-octahedral complexes. This results in iodido complexes which are more potent and more selective toward cancer cell lines, are not cross-resistant with platinum drugs used in the clinic, show a high selectivity for membrane binding, are not dependent on p53 for activity, induce a high incidence of late-stage apoptosis, and possess potency which is greatly increased by a low dose of the redox modulator L-BSO. Our findings illustrate the exciting potential which metal complexes offer for the design of novel anticancer agents.

■ EXPERIMENTAL SECTION

$RuCl_3 \cdot 3H_2O$ was purchased from Precious Metals Online (PMO pty Ltd.). All solvents (acetone, methanol, and ether) were obtained from commercial sources such as Fisher Scientific and Sigma-Aldrich and were used without further purification; ethanol was obtained from the same suppliers but dried over Mg/I_2 before use. α-Phellandrene was also purchased from Sigma Aldrich. Deuterated solvents were purchased from Cambridge Isotopes Limited. ICP-MS standards (Ru, Os) were obtained from Inorganic Ventures. For the biological experiments, RPMI-1640, DMEM, McCoy 5A media, as well as fetal bovine serum, L-glutamine, penicillin/streptomycin mixture, trypsin, trypsin/EDTA, and phosphate buffered saline (PBS) were purchased from PAA Laboratories GmbH. CDDP ($\geq$99.9%), OXA ($\geq$98.9%), trichloroacetic acid ($\geq$99%), sulforhodamine B (75%), sodium phosphate monobasic monohydrate ($\geq$99%), sodium phosphate dibasic heptahydrate ($\geq$99%), acetic acid ($\geq$99%), L-BSO ($\geq$97%), staurosporine, PI ($\geq$94%), and RNase A were obtained from Sigma Aldrich together with the Annexin V-FITC Apoptosis Detection Kit for flow cytometry. Caspase activity was determined using the Caspase-3 Colorimetric Assay Kit from Cambridge Biosciences. Cell fractionation was carried out using FractionPREP Kit from BioVision.

NMR data (^{1}H, ^{13}C and 2D experiments) were acquired using 5 mm NMR tubes in the NMR Spectroscopy Facility of Warwick University on either a 500 MHz spectrometer Bruker DRX-500 or a 600 MHz Bruker AVA spectrometer; experiments were carried out at 298 K unless otherwise stated. ^{1}H NMR chemical shifts were internally referenced to DMSO-d_6 (2.50 ppm) or 1,4-dioxane (3.71 ppm, for samples in D_2O). Typically, the spectral width was 20 ppm for ^{1}H NMR and 200 ppm for ^{13}C NMR experiments. Spectra were processed using Bruker Topspin 2.1. Elemental analysis (percentages of C, H and N) was carried out on a CE-440 Exeter elemental analyzer by the Warwick Analytical Service. Mass spectrometry data were obtained on methanolic solutions (50% MeOH, 50% H_2O) on a Bruker Esquire 2000 instrument with electrospray as the ionization method. Usually experiments were based on scanning a range of up to 1000 m/z for positive ions; the cone voltage and source temperature were varied depending on the sample.

Synthesis of Complex 1. Ruthenium p-cymene dimer $[(\eta^6$-p-cymene)RuCl_2]_2 (100 mg, 0.16 mmol) was dissolved in methanol (5 mL). Two mol equiv of p-Impy−NMe$_2$ were added (74 mg, 0.33 mmol). The reaction mixture was left at ambient temperature with constant stirring for 5 h. After this time, 5 mol equiv of NH_4PF_6 were added to the mixture, followed by stirring for a further hour. The solid precipitate was filtered off under vacuum and recrystallized. (84%). ^{1}H NMR (500 MHz; DMSO-d_6) δ 0.99 (dd, J = 1.1, 2.3, 6.9, 9.3 Hz, 6H), 2.20 (s, 3H), 2.46 (m, 1H), 3.12 (s, 6H), 5.62 (2H), 5.78 (d, J = 7.3 Hz, 1H), 6.11 (d, J = 6.7 Hz, 1H), 6.89 (d, J = 8.4 Hz, 2H), 7.70 (d, J = 9.0 Hz, 2H), 7.81 (t, J = 7.9, 14.1 Hz, 1H), 8.18 (d, J = 6.7 Hz, 1H), 8.26 (t, J = 7.3, 14.7 Hz, 1H), 8.78 (s, 1H), 9.51(d, J = 4.0 Hz, 1H); (m/z) $[M]^+$ calcd for $C_{22}H_{29}N_3ClRu$, 472.01; found. 472.0. Analysis (calcd, found for $C_{22}H_{29}N_3ClF_6PRu$): C (42.83, 42.68), H (4.74, 4.81), N (6.81, 6.74). Purity of this complex was determined to be >98% by elemental analysis and HPLC.

Synthesis of Complex 2. Ruthenium p-cymene dimer $[(\eta^6$-p-cymene)RuI_2]_2 (150 mg, 0.19 mmol) was dissolved in methanol (5 mL). Two mol equiv of p-Impy−NMe$_2$ were added (89 mg, 0.38 mmol). The reaction mixture was left at ambient temperature with constant stirring for 5 h. After this time, 5 mol equiv of NH_4PF_6 were added to the mixture, followed by stirring for a further hour. The solid precipitate was filtered off under vacuum and recrystallized (64%). ^{1}H NMR (500 MHz; DMSO-d_6) δ 1.00 (dd, J = 7.3, 12.2, 18.1 Hz, 6H), 2.45 (s, 3H), 2.56 (m, 1H), 3.07 (s, 6H), 5.59 (d, J = 8.8 Hz, 1H), 5.65 (d, J = 8.1 Hz, 1H), 5.77 (d, J = 8.8 Hz, 1H), 6.08 (d, J = 8.1 Hz, 1H), 7.73 (d, J = 3.8, 6.6 Hz, 1H), 7.77 (d, J = 10.8 Hz, 1H), 8.19 (t, J = 7.9, 14.1 Hz, 1H), 8.21 (d, J = 7.5 Hz, 1H), 8.72 (s, 1H), 9.48 (d, J = 4.8 Hz, 1H); (m/z) $[M]^+$ calcd for $C_{22}H_{29}N_3IRu$, 587.48; found 587.4. Analysis (calcd, found for $C_{24}H_{29}N_3F_6IPRu$): C (39.36, 39.24), H (3.99, 3.98), N (5.74, 5.71). Purity of this complex was determined to be >98% by elemental analysis, and HPLC.

ICP-MS. An Agilent 7500 series ICP-MS instrument was used. Samples and metal standards (Ru/Os; fresh for each experiment) were prepared in doubly deionized water (DDW) with 5% HNO_3. The concentrations used for the calibration curves were 0, 5, 10, 50, 200, 500, 1×10^3, 5×10^3, 10×10^3, 50×10^3, and 200×10^3 ppt. The isotopes detected were ^{101}Ru and ^{189}Os, and readings were made in duplicate (He gas and no-gas mode).

Cell Culture. A2780 human ovarian carcinoma, A549 human Caucasian lung carcinoma, HCT116 human colon carcinoma, MCF7 human Caucasian breast carcinoma, and MRC5 human fetal lung fibroblasts were obtained from the European Collection of Cell Cultures (ECACC) and used between passages 5 and 18. Modified cell lines HCT116Ox and HCT116p53−/−, which have the tumor suppressor p53 knocked out, were kindly provided by R. Sharma from Oxford University and J. Cherry from Johns Hopkins International Medical Center, respectively. A2780 ovarian and MRC5 cells were grown in Roswell Park Memorial Institute medium (RPMI-1640), A549 and MCF7 cells in Dulbecco's Modified Eagle Medium (DMEM), and HCT116 cells and its derived cell lines in McCoy's Modified 5A Medium. All media were supplemented with 10% of fetal calf serum, 1% of 2 mM glutamine, and 1% penicillin/streptomycin. All cells were grown as adherent monolayers at 310 K in a 5% CO_2 humidified atmosphere.

In Vitro Growth Inhibition Assay. Briefly, 5000 cells were seeded per well in 96-well plates. The cells were preincubated in drug-free media at 310 K for 48 h before adding different concentrations of the compounds to be tested. The drug exposure period was 24 h. After this, supernatants were removed by suction and each well was washed with PBS. A further 72 h was allowed for the cells to recover in drug-free medium at 310 K. The SRB assay[57] was used to determine cell viability. Absorbance measurements of the solubilized dye (on a BioRad iMark microplate reader using a 470 nm filter) allowed the determination of viable treated cells compared to untreated controls. IC_{50} values (concentrations which caused 50% of cell death) were determined as duplicates of triplicates in two independent sets of experiments, and their standard deviations were calculated.

Metal Accumulation in Cancer Cells. Cell accumulation studies for complexes 1−6 were conducted on A2780 ovarian cells. Briefly, 4 $\times 10^6$ cells were seeded on a Petri dish. After 24 h of preincubation time in drug-free medium at 310 K, the complexes were added to give final concentrations equal to $IC_{50}/3$ and a further 24 h of drug exposure was allowed. After this time, cells were treated with trypsin, counted, and cell pellets were collected. Each pellet was digested overnight in concentrated nitric acid (73%) at 353 K; the resulting solutions were diluted with double-distilled water to a final concentration of 5% HNO_3, and the amount of Ru/Os taken up by the cells was determined by ICP-MS. These experiments did not include any cell recovery time in drug-free media; they were carried out in triplicate, and the standard deviations were calculated.

Metal Distribution in Cancer Cells. Cell pellets were obtained as described above and were fractionated using the FractionPREP kit from BioVision according to the supplier's instructions. Each sample was digested overnight in concentrated nitric acid (73%), and the amount of Ru/Os taken up by the cells was determined by ICP-MS.

These experiments were all carried out in triplicate, and the standard deviations were calculated.

Cell Cycle Analysis. A2780 cells, 1.5×10^6 per well, were seeded in a 6-well plate. Cells were preincubated in drug-free media at 310 K for 24 h, after which drugs were added at equipotent concentrations of $IC_{50}/3$. After 24 h of drug exposure, supernatants were removed by suction and cells were washed with PBS. Finally, cells were harvested using trypsin. DNA staining was achieved by resuspending the cell pellets in PBS containing propidium iodide (PI) and RNase A. Cell pellets were resuspended in PBS before being analyzed in a Becton Dickinson FACScan flow cytometer using excitation of DNA-bound PI at 536 nm, with emission at 617 nm. Data were processed using Flowjo software.

Role of p53-Activated Apoptotic Pathway. IC_{50} values for complexes **1−6** were determined as described above in the HCT116p53−/− cell line, which has the tumor suppressor p53 knocked out.

Induction of Apoptosis. Flow cytometry analysis of apoptotic populations of A2780 cells caused by exposure to complexes **1−6** was carried out using the Annexin V-FITC Apoptosis Detection Kit (Sigma Aldrich) according to the supplier's instructions. For positive-apoptosis controls, A2780 cells were exposed to staurosporine (1 μg/mL) for 2 h. Cells for apoptosis studies were used with no previous fixing procedure as to avoid nonspecific binding of the annexin V-FITC conjugate.

Activation of Caspase 3. Colorimetric analysis of caspase 3 activation in A2780 ovarian cells exposed to complexes **1−6** was carried out using the Caspase-3/CPP32 Colorimetric assay Kit (Cambridge Biosciences) according to the supplier's instructions. The resulting solutions were read in an absorbance plate reader at 410 nm (free p-NA). Samples were analyzed in triplicate, and standard deviations were calculated. For positive activation of caspase 3, A2780 cells were exposed to staurosporine (1 μg/mL) for 2 h.

ASSOCIATED CONTENT

Ⓢ Supporting Information
Synthesis. HPLC analysis for the Cl to I conversion of complex **1** and computational details for complexes **1−6**. Metal distribution, cell cycle analysis, distribution of apoptotic populations, activation of caspase 3, and antiproliferative activity modulation by the use of L-BSO for complexes **1−6** in A2780 cells. This material is available free of charge via the Internet at http://pubs.acs.org.

AUTHOR INFORMATION

Corresponding Author
*Phone: (+44) 024 7652 3818. Fax: +44-24-76523819. E-mail: P.J.Sadler@warwick.ac.uk.

Author Contributions
I.R.C. designed and carried out chemical and biological experiments, analyzed and interpreted data, L.S. carried out the DFT calculations, and P.J.S. designed experiments and analyzed and interpreted data. All authors contributed to the writing of the manuscript.

Notes
The authors declare the following competing financial interest(s): P.J.S. is named inventor on a patent application relating to the osmium complexes used in this work filed by the University of Warwick.

ABBREVIATIONS USED
CDDP, cisplatin; OXA, oxaliplatin; L-BSO, L-buthionine sulfoxime; EPSs, electrostatic potential surfaces; ROS, reactive oxygen species; SSB, single strand breaks; MMR, mismatch repair; PI, propidium iodide; mDNA, mitochondrial DNA; GSH, glutathione

REFERENCES
(1) Kartalou, M.; Essigmann, J. M. Mechanisms of resistance to cisplatin. *Mutat. Res.* **2001**, *478*, 23−43.
(2) Kelland, L. The resurgence of platinum-based cancer chemotherapy. *Nature Rev. Cancer* **2007**, *7*, 573−584.
(3) Howell, S. B.; Safaei, R.; Larson, C. A.; Sailor, M. J. Copper transporters and the cellular pharmacology of the platinum-containing cancer drugs. *Mol. Pharmacol.* **2010**, *77*, 887−894.
(4) Todd, R. C.; Lippard, S. J. Inhibition of transcription by platinum antitumor compounds. *Metallomics* **2009**, *1*, 280−291.
(5) Bergamo, A.; Gaiddon, C.; Schellens, J. H.; Beijnen, J. H.; Sava, G. Approaching tumour therapy beyond platinum drugs: status of the art and perspectives of ruthenium drug candidates. *J. Inorg. Biochem.* **2012**, *106*, 90−99.
(6) Scolaro, C.; Bergamo, A.; Brescacin, L.; Delfino, R.; Cocchietto, M.; Laurenczy, G.; Geldbach, T. J.; Sava, G.; Dyson, P. J. In vitro and in vivo evaluation of ruthenium(II)−arene PTA complexes. *J. Med. Chem.* **2005**, *48*, 4161−4171.
(7) Morris, R. E.; Aird, R. E.; Murdoch, P. D. S.; Chen, H.; Cummings, J.; Hughes, N. D.; Parsons, S.; Parkin, A.; Boyd, G.; Jodrell, D. I.; Sadler, P. J. Inhibition of cancer cell growth by ruthenium(II)−arene complexes. *J. Med. Chem.* **2001**, *44*, 3616−3621.
(8) Schäfer, S.; Ott, I.; Gust, R.; Sheldrick, W. S. Influence of the Polypyridyl (pp) Ligand Size on the DNA Binding Properties, Cytotoxicity and Cellular Uptake of Organoruthenium(II) Complexes of the Type $[(\eta^6\text{-}C_6Me_6)Ru(L)(pp)]^{n+}$ $[L=Cl, n = 1; L=(NH_2)_2CS, n = 2]$. *Eur. J. Inorg. Chem.* **2007**, 3034−3046.
(9) Antonarakis, E. S.; Emadi, A. Ruthenium-based chemotherapeutics: are they ready for prime time? *Cancer Chemother. Pharm.* **2010**, *66*, 1−9.
(10) Bratsos, I.; Jedner, S.; Gianferrara, T.; Alessio, E. Ruthenium Anticancer Compounds: Challenges and Expectations. *Chimia* **2007**, *61*, 692−697.
(11) Cleare, M.; Hoieschele, J. D. Studies on the antitumor activity of group VIII transition metal complexes. Part I. Platinum(II) complexes. *Bioinorg. Chem.* **1973**, *2*, 187−210.
(12) Messori, L.; Cubo, L.; Gabbiani, C.; Álvarez-Valdés, A.; Michelucci, E.; Pieraccini, G.; Ríos-Luci, C.; León, L. G.; Padrón, J. M.; Navarro-Ranninger, C.; Casini, A.; Quiroga, A. G. Reactivity and biological properties of a series of cytotoxic $PtI_2(amine)_2$ complexes, either cis or trans configured. *Inorg. Chem.* **2012**, *51*, 1717−1726.
(13) Wang, F.; Habtemariam, A.; Van der Geer, E.; Fernández, R.; Melchart, M.; Deeth, R. J.; Aird, R.; Guichard, S.; Fabbiani, F. P.; Lozano-Casal, P.; Oswald, I. D. H.; Jodrell, D. I.; Parsons, S.; Sadler, P. J. Controlling ligand substitution reactions of organometallic complexes: tuning cancer cell cytotoxicity. *Proc. Natl. Acad. Sci. U. S. A.* **2005**, *102*, 18269−18274.
(14) Peacock, A. F. A.; Habtemariam, A.; Fernández, R.; Walland, V.; Fabbiani, F.; Parsons, S.; Aird, R. E.; Jodrell, D. I.; Sadler, P. J. Tuning the reactivity of osmium(II) and ruthenium(II) arene complexes under physiological conditions. *J. Am. Chem. Soc.* **2006**, *128*, 1739−1748.
(15) Bruijnincx, P. C.; Sadler, P. J. Controlling platinum, ruthenium and osmium reactivity for anticancer drug design. *Adv. Inorg. Chem.* **2009**, *61*, 1−62.

(16) Yan, Y. K.; Melchart, M.; Habtemariam, A.; Sadler, P. J. Organometallic chemistry, biology and medicine: ruthenium arene anticancer complexes. *Chem. Commun.* **2005**, 4764−4776.

(17) Süss-Fink, G. Arene ruthenium complexes as anticancer agents. *Dalton Trans.* **2010**, *39*, 1673−1688.

(18) Melchart, M.; Habtemariam, A.; Parsons, S.; Sadler, P. J. Chlorido- aqua- ethylguanine and ethyladenine adducts of cytotoxic ruthenium arene complexes containing O,O-chelating ligands. *J. Inorg. Biochem.* **2007**, *101*, 1903−1912.

(19) Wang, F.; Xu, J.; Wu, K.; Weidt, S. K.; Mackay, C. L.; Langridge-Smith, P. R. R.; Sadler, P. J. Competition between glutathione and DNA oligonucleotides for ruthenium(ii) arene anticancer complexes. *Dalton Trans.* **2013**, DOI: 10.1039/c2dt32091f.

(20) Wang, F.; Weidt, S.; Xu, J.; Mackay, C. L.; Langridge-Smith, P. R. R.; Sadler, P. J. Identification of clusters from reactions of ruthenium arene anticancer complex with glutathione using nanoscale liquid chromatography Fourier transform ion cyclotron mass spectrometry combined with (18)O-labeling. *J. Am. Soc. Mass Spectrom.* **2008**, *19*, 544−549.

(21) Dougan, S. J.; Habtemariam, A.; McHale, S. E.; Parsons, S.; Sadler, P. J. Catalytic organometallic anticancer complexes. *Proc. Natl. Acad. Sci. U. S. A.* **2008**, *105*, 11628−11633.

(22) Fu, Y.; Romero, M. J.; Habtemariam, A.; Snowden, M. E.; Song, L.; Clarkson, G. J.; Qamar, B.; Pizarro, A. M.; Unwin, P. R.; Sadler, P. J. The contrasting chemical reactivity of potent isoelectronic iminopyridine and azopyridine osmium(II) arene anticancer complexes. *Chem. Sci.* **2012**, *3*, 2485−2493.

(23) Chu, G. Cellular responses to cisplatin. *J. Biol. Chem.* **1994**, *269*, 787−790.

(24) McLean, A. D.; Chandler, G. S. Contracted Gaussian basis sets for molecular calculations. I. Second row atoms, Z = 11−18. *J. Chem. Phys.* **1980**, *72*, 5639−5648.

(25) Hay, P. J.; Wadt, W. R. Ab initio effective core potentials for molecular calculations. Potentials for the transition metal atoms Sc to Hg. *J. Chem. Phys.* **1985**, *82*, 270−283.

(26) Perdew, J. P.; Burke, K.; Ernzerhof, M. Generalized gradient approximation made simple. *Phys. Rev. Lett.* **1996**, *77*, 3865−3868.

(27) Teis, D.; Huber, L. The odd couple: signal transduction and endocytosis. *Cell. Mol. Life Sci.* **2003**, *60*, 2020−2033.

(28) Jungwirth, U.; Kowol, C. R.; Keppler, B. K.; Hartinger, C. G.; Berger, W.; Heffeter, P. Anticancer activity of metal complexes: involvement of redox processes. *Antioxid. Redox Signaling* **2011**, *15*, 1085−1127.

(29) Wondrak, G. T. Redox-directed cancer therapeutics: molecular mechanisms and opportunities. *Antioxid. Redox Signaling* **2009**, *11*, 3013−3069.

(30) Kovacic, P. Unifying mechanism for anticancer agents involving electron transfer and oxidative stress: clinical implications. *Med. Hypotheses* **2007**, *69*, 510−516.

(31) Faivre, S. DNA strand breaks and apoptosis induced by oxaliplatin in cancer cells. *Biochem. Pharmacol.* **2003**, *66*, 225−237.

(32) Helleday, T.; Petermann, E.; Lundin, C.; Hodgson, B.; Sharma, R. DNA repair pathways as targets for cancer therapy. *Nature Rev. Cancer* **2008**, *8*, 193−204.

(33) Ngamkitidechakul, C.; Jaijoy, K.; Hansakul, P.; Soonthornchareonnon, N.; Sireeratawong, S. Antitumour effects of *Phyllanthus emblica* L.: induction of cancer cell apoptosis and inhibition of in vivo tumour promotion and in vitro invasion of human cancer cells. *Phytother. Res.* **2010**, *24*, 1405−1413.

(34) Sharma, P.; Farrell, T.; Patterson, M. S.; Singh, G.; Wright, J. R.; Sur, R.; Rainbow, A. J. In vitro survival of nonsmall cell lung cancer cells following combined treatment with ionizing radiation and photofrin-mediated photodynamic therapy. *Photochem. Photobiol.* **2009**, *85*, 99−106.

(35) Romero-Canelón, I.; Pizarro, A. M.; Habtemariam, A.; Sadler, P. J. Contrasting cellular uptake pathways for chlorido and iodido iminopyridine ruthenium arene anticancer complexes. *Metallomics* **2012**, *4*, 1271−1279.

(36) Schütze, S.; Tchikov, V.; Schneider-Brachert, W. Regulation of TNFR1 and CD95 signalling by receptor compartmentalization. *Nature Rev. Mol. Cell Biol.* **2008**, *9*, 655−662.

(37) Tan, K. H.; Hunziker, W. Compartmentalization of FAS and FAS ligand may prevent auto- or paracrine apoptosis in epithelial cells. *Exp. Cell Res.* **2003**, *284*, 281−288.

(38) Zheng, H.; Hu, W.; Yu, D.; Shen, D. Y.; Fu, S.; Kavanagh, J. J.; Wei, C.; Yang, D. J. Diammine dicarboxylic acid platinum enhances cytotoxicity in platinum-resistant ovarian cancer cells through induction of apoptosis and S-phase cell arrest. *Pharm. Res.* **2008**, *25*, 2272−2282.

(39) Tan, C.; Wu, S.; Lai, S.; Wang, M.; Chen, Y.; Zhou, L.; Zhu, Y.; Lian, W.; Peng, W.; Ji, L.; Xu, A. Synthesis, structures, cellular uptake and apoptosis-inducing properties of highly cytotoxic ruthenium−Norharman complexes. *Dalton Trans.* **2011**, *40*, 8611−8621.

(40) Liu, H.; Li, Y.; Raisch, K. Clotrimazole induces a late G1 cell cycle arrest and sensitizes glioblastoma cells to radiation in vitro. *Anti-Cancer Drugs* **2010**, *21*, 841−849.

(41) Demidenko, Z. N.; Kalurupalle, S.; Hanko, C.; Lim, C.; Broude, E.; Blagosklonny, M. V Mechanism of G1-like arrest by low concentrations of paclitaxel: next cell cycle p53-dependent arrest with sub G1 DNA content mediated by prolonged mitosis. *Oncogene* **2008**, *27*, 4402−4410.

(42) Moll, U. M.; Concin, N. p53 in Human Cancer—Somatic and Inherited Mechanisms. In *The p53 Tumor Suppressor Pathway and Cancer*; Protein Reviews; Springer: New York, 2005; Vol. 2, pp 115−154

(43) Post, S. M.; Quintás-Cardama, A.; Lozano, G. Regulation of p53 activity and associated checkpoint controls. In *Checkpoint Controls and Targets in Cancer Therapy*; Siddik, Z. H., Ed.; Springer Science: New York, 2010; pp 171−188.

(44) Wang, S.; El Deiry, W. S. p53, cell cycle arrest and apoptosis. In *25 Years of p53 Reseacrh*; Springer: Dordrecht, 2007; pp 141−163.

(45) Chatterjee, S.; Kundu, S.; Bhattacharyya, A.; Hartinger, C. G.; Dyson, P. J. The ruthenium(II)−arene compound RAPTA-C induces apoptosis in EAC cells through mitochondrial and p53-JNK pathways. *J. Biol. Inorg. Chem.* **2008**, *13*, 1149−1155.

(46) Hayward, R. L.; Schornagel, Q. C.; Tente, R.; Macpherson, J. S.; Aird, R. E.; Guichard, S.; Habtemariam, A.; Sadler, P. J.; Jodrell, D. I. Investigation of the role of Bax, p21/Waf1 and p53 as determinants of cellular responses in HCT116 colorectal cancer cells exposed to the novel cytotoxic ruthenium(II) organometallic agent, RM175. *Cancer Chemother. Pharm.* **2005**, *55*, 577−583.

(47) Quinn, P. J. Plasma Membrane Phospholipid Asymmetry. *Subcell. Biochem.* **2002**, *36*, 1−25.

(48) Salvesen, G. S.; Riedl, S. J. Caspase mechanisms. *Adv. Exp. Med. Biol.* **2008**, *615*, 13−23.

(49) Gurtu, V.; Kain, S. R.; Zhang, G. Fluorometric and colorimetric detection of caspase activity associated with apoptosis. *Anal. Biochem.* **1997**, *102*, 98−102.

(50) Chen, T.; Liu, Y.; Zheng, W. J.; Liu, J.; Wong, Y. S. Ruthenium polypyridyl complexes that induce mitochondria-mediated apoptosis in cancer cells. *Inorg. Chem.* **2010**, *49*, 6366−6368.

(51) Hara, K.; Kasahara, E.; Takahashi, N.; Konishi, M.; Inoue, J.; Jikumaru, M.; Kubo, S.; Okamura, H.; Sato, E.; Inoue, M. Mitochondria determine the efficacy of anticancer agents that interact with DNA but not the cytoskeleton. *J. Pharmacol. Exp. Ther.* **2011**, *337*, 838−845.

(52) Chen, H. H. W.; Kuo, M. T. Role of glutathione in the regulation of cisplatin resistance in cancer chemotherapy. *Met. Based Drugs* **2010**, DOI: 10.1155/2010/430939.

(53) Hall, M. D.; Okabe, M.; Shen, D. W.; Liang, X. X.; Gottesman, M. M. The role of cellular accumulation in determining sensitivity to platinum-based chemotherapy. *Annu. Rev. Pharmacol. Toxicol.* **2008**, *48*, 495−535.

(54) Trachootham, D.; Zhang, W.; Huang, P. Oxidative Stress and Drug Resistance in Cancer. In *Drug Resistance in Cancer Cells*; Siddik, Z. H., Mehta, K., Eds.; Springer: New York, 2009; pp 137−175.

(55) Anderson, C. P.; Reynolds, C. P. Synergistic cytotoxicity of buthionine sulfoximine (BSO) and intensive melphalan (L-PAM) for neuroblastoma cell lines established at relapse after myeloablative therapy. *Bone Marrow Transplant.* **2002**, *30*, 135−140.

(56) Shnyder, S. D.; Fu, Y.; Habtemariam, A.; Rijt, S. H.; Van; Cooper, P.; Loadman, P. M.; Sadler, P. J. Anti-colorectal cancer activity of an organometallic osmium arene azopyridine complex. *MedChem-Comm* **2011**, *2*, 666−668.

(57) Vichai, V.; Kirtikara, K. Sulforhodamine B colorimetric assay for cytotoxicity screening. *Nature Protoc.* **2006**, *1*, 1112−1116.